Intelligent Automation And Soft Computing, 2019
Copyright © 2019, TSI® Press
Vol. 25, no. 4, 745–753
https://doi.org/10.31209/2019.100000078

Storage-Based Control Loop for AGC to Mitigate the Tie-Lines Power Excursion Between Areas

Shengqi Zhang, Bei Yuan, Jianfeng Zhao

School of Electrical Engineering, Southeast University, 2 Sipailou Xuwu District, Nanjing, China)

ABSTRACT

With the current trend of deregulation, more power exchange between GENCOs and DISCOs in different areas exists in the power system. To mitigate the unscheduled power exchange meets the common interests of GENCOs and DISCOs, and avoids the power over-loading on tie-lines. However, in the current control performance standards (CPS), frequency deviations have priority in the conventional automatic generation control (C-AGC). Thus, a storage-based tie-line control loop (STCL) on the basis of C-AGC (STCL-AGC) is proposed in this paper, which makes a better tradeoff in the recovery of the frequency deviations and the unscheduled power exchange. In STCL-AGC, utility-scaled battery energy storage systems (BESS) in neighboring areas are referred to supply and consume the same amount of power and respond to the unscheduled power exchange. Meanwhile, as the operation of BESS is not always positive on the recovery of frequency deviations and area control error (ACE), CPS are involved to ensure the practical use of STCL-AGC. At last, in a two-area interconnected power system case, promising results are shown that the unscheduled power exchange is mitigated effectively by STCL-AGC with small sizes of BESS.

KEY WORDS: Automatic generation control, area control error, battery energy storage system, control performance standards, unscheduled tie-line power.

1 INTRODUCTION

IN the deregulated power system operation, GENCOs do not always cooperate with TRANCOs, but have contracts with DISCOs as power suppliers methioned by Christie, et. al. (2007). Meanwhile, as the extension of the interconnected power system, GENCOs and DISCOs are often located in different control areas, and transfer power through tie-lines. Also, as all generators are under synchronous operation with the primary frequency control, the unscheduled power exchange (ΔP_{tie}) on tie-lines is unavoidable in the balance of the generation and load. In some cases, the power over-loading on tie-lines threatens the safety of the interconnected power system. Thus, to mitigate ΔP_{tie} in the premise of the frequency stability gets more attention.

In current power system, the conventional automatic generation control (C-AGC) is the essential controller to make the target frequency and the scheduled power exchange around the nominal values. To achieve those dual objectives in AGC, area control errors (ACE) which combines the frequency deviations (Δf) and the unscheduled power exchanges (ΔP_{tie}) is used as the input signal. In practical, PI-based AGC with online parameters tuning has been widely used written by Mohanty, et. al. (2016) and Mercier, et. al. (2009). Also, many researches have been done to get better PI parameters. For example, an iterative linear matrix inequalities algorithm was used by Bevrani, et. al. (2004) and Ma, et. al. (2017). Farahani, et. al. (2012) and Tan (2010) introduce PID-based AGC with the chaotic optimization algorithm and the unified tuning algorithm. Meanwhile, the decentralized sliding mode method proposed by Mi, et. al. (2013), the adaptive gain controller proposed by Olmos, et. al. (2004) and the genetic algorithms proposed by Rerkpreedapong, et. al. (2003) and Kung, et. al. (1998) are also used to improve AGC.

Furthermore, AGC is not significantly improved until the involvement of energy storage systems (ESS), because ESS act as the fast response generators with flexible control performance proposed by Delille, et. al. (2012) and Sui, et. al. (2014). For example, battery

CONTACT Shengqi Zhang shengqi_zhang8816@163.com

energy storage systems (BESS) respond to Δf proposed by Chen, et. al. (2016), Pan, et. al. (2016) and Miao,. et. al. (2015). Moreover, BESS can be also used for AGC to improve the recovery of Δf and ΔP_{tie} effectively as methioned by Cheng, et. al. (2014), Sharma, et. al. (2014) and Tabarez, et. al. (2016). Meanwhile, those papers also indicate BESS must be wisely used as their high operating cost and limited capacities. In detail, BESS take the AGC responsibility in proportion to their power reserve in the total power reserve as Cheng, et. al. (2014). A low-pass filter is used in Sharma, et. al. (2014), and BESS are applied only when Δf is large. Also, the involvement of BESS for AGC is decided by monitoring the system index as Tabarez, et. al. (2016).

According to those research, each area is under the independent control, and the stability of Δf is the main factor in the evaluation of the AGC performance. Also, ΔP_{tie} sometimes is encouraged in the recovery of Δf, and is finally mitigated owning to the recovery of Δf. Meanwhile, the involvement of ESS essentially makes the recovery of Δf faster methioned in Kottick, et. al. (1993). Thus, the fluctuations of ΔP_{tie} are not get enough attention in the process of the C-AGC, although AGC is theoretically a coordinated control for Δf and ΔP_{tie}.

In this paper, a storage-based tie-line control loop (STCL) on the basis of the C-AGC (STCL-AGC) is proposed. BESS in neighboring areas as the asynchronous power system participators operate in pairs under the coordinated control. In detail, BESS in both ends of the tie-lines supply and consume power at the same time by responding to the fluctuations of ΔP_{tie}, and their participation is based on Δf and *ACE* in neighboring areas.

In this way, the required sizes of BESS are effectively decreased, because BESS do not compensate the mismatches between load and generation. Meanwhile, the performance of AGC is improved as BESS are with the fast response time. Also, ΔP_{tie} is mitigated in the process of the recovery of Δf. Furthermore, the area control performance standards (CPS) are evaluated in real time, which ensures the practical use of STCL-AGC. To sum up, a better tradeoff in the control of Δf and ΔP_{tie} is achieved in STCL-AGC.

2 EFFECTS OF CPS IN C-AGC

AGC in practical does not simply bring ACE to zero, and some actual situations such as minimizing the fuel cost, minimizing equipment wear and tear are considered. CPS, which are drawn by North American Electric Reliability (NERC) in 1997, are regarded as fair criteria to evaluate the AGC performance of each area, and have been widely used in many countries. CPS consist of two indexes namely CPS1 and CPS2, and the qualified CPS of an area mean that CPS1 and CPS2 are more than 100% and 90% respectively recorded in Avila, et. al. (2016). More specifically, CPS1 is based on the 1 minute average values of Δf and *ACE* marked as ΔF_1 and ACE_1 in (1) and (2), and CPS2 is based on the 10 minutes average values of *ACE* marked as ACE_{10} in (3) and (4). In addition, B is the frequency bias coefficient in MW/0.1Hz, which is a **Positive Value** and cannot be changed dynamically, and ϵ_1 and L_{10} are fixed parameters set by ISO.

$$CF1 = \frac{1}{\epsilon_1^2}\left\{\frac{ACE}{-10B}\right\}_1 \times \Delta F_1 \tag{1}$$

$$CPS1 = 100\%(2 - AVG\{CF1\}) \tag{2}$$

$$CF2 = \frac{|ACE_{10}|}{L_{10}} \tag{3}$$

$$CPS2 = 100\%\left(1 - \frac{\text{No.of intervals } CP2>1}{\text{Total No.of intervals}}\right) \tag{4}$$

CPS1 indicates the performance of AGC in a short period. In detail, ΔF_1 and ACE_1 are with the opposite signs in the second and forth quadrants, which means *ACE* is positive to the recovery of Δf. In other words, ΔP_{tie} is positive to the recovery of Δf, and AGC generators do not take action to mitigate ΔP_{tie} according to CPS1. In this way, the wear and tear of generators decreases.

On the contrary, ΔF_1 and ACE_1 are with the same signs in the first and third quadrants, and AGC generators must take action to avoid the CPS1 deterioration. Thus, Δf is effectively constrained by CPS1 in the C-AGC.

Furthermore, CPS2 seems to restraint *ACE* only, but is essentially the constraints of ΔP_{tie}, as Δf has been already amended in CPS1. However, 10 minutes which is relatively a large time scale, provide a large toleration in the control of ΔP_{tie} in AGC.

Therefore, under the constrains of CPS, the C-AGC enhances the frequency stability of the interconnected power system and decreases the redundant adjustment of generators, but ignores the mitigation of ΔP_{tie} in some cases. More strict CPS2 is a way to mitigate ΔP_{tie}, but sometimes harms to the power supports between areas. Thus, STCL-AGC proposed in this paper is considered as a flexible supplementary control loop on the basis of C-AGC to mitigate ΔP_{tie} in the premise of the frequency stability. The power over-loading on the tie-line is avoided in the STCL-AGC, and a better tradeoff is made in the control of Δf and ΔP_{tie}.

3 FRAMEWORK OF STCL-AGC IN NEIGHBORING AREAS

TWO neighboring areas marked as *Area i* and *Area j* are connected by the tie-line with the scheduled power exchange from *Area i* to *Area j*, as Figure 1, and each area is equipped with a utility-scaled BESS (namely $BESS_i$ and $BESS_j$). Compared with C-AGC in Dong, et. al. (2017), an extra control loop for the pair of BESS named STCL is included in STCL-AGC.

Specifically, BESS in neighboring areas are always under the coordinated control to respond the excursion of ΔP_{tie} and offset the unscheduled power exchange.

The framework of STCL consists of 'CPS Index block', 'Charging / Discharging (+/-) Index block' and 'BESS Operation block'. At the beginning, 'CPS Index block' calculates the possible participation factors (K_{Bi}^* and K_{Bj}^*) of BESS in each area to mitigate ΔP_{tie}, according to CPS1. In the following step, because BESS operate in pairs, the same participation factor (K_B) is decided by '+/- Index block', as well as the operation mode (charging (-) or discharging (+)) for each BESS. At last, BESS characteristics such as the rated power, the rated capacity and SoC are concerned in 'BESS Operation block'.

In this way, BESS do not take responsibility to compensate the power mismatch between generation and load. However, as BESS are with fast response time, they still replace the generators in a short period before the generators finish their AGC. Meanwhile, those three blocks operate in real time, and ΔP_{tie} is mitigated without the exceeding of CPS. Thus, the AGC performance is improved including the mitigation of ΔP_{tie}, and the sizes of BESS are effectively decreased. More details of STCL are further discussed in the following parts.

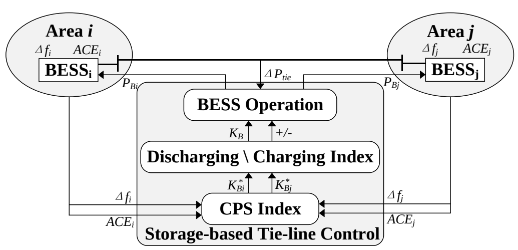

Figure 1. STCL in two neighboring areas.

3.1 CPS Index Block

The process of 'CPS Index Block' is shown as the left part of Figure 2. The inputs of the block are Δf and ACE of each area marked as Δf_i, Δf_j, ACE_i and ACE_j, and the outputs K_{Bi}^* and K_{Bj}^* are calculated independently. Specifically, K_B^* indicates the operation of BESS for mitigating ΔP_{tie}, when the recovery of ΔP_{tie} is against the recovery of Δf.

Specifically, CPS1 of the area is more than 200%, when Δf and ACE are with opposite signs. In this case, BESS completely focus on mitigating ΔP_{tie} without considering the recovery of Δf, and $K_B^* = K_{B.max}$. Also, if Δf and ACE are with the same sign, but CPS1 is more than 150. The operation of BESS is required to balance the recovery of Δf and ΔP_{tie}, and $K_B^* = \frac{200-CPS1}{50} \cdot K_{B.max}$. Otherwise, the operation of BESS must be benefit to the recovery of Δf, and $K_B^* = 0$. Thus, 'CPS Index Block' ensures the practical use of STCL-AGC as sanctions are applied when the control area fails to meet CPS.

3.2 Charging/discharging Index block

The 'discharging / charging/ (+/-) Index block' is the center of STCL, and the process is shown as the middle part of Figure 2. The block decides the participation factor K_B for a pair of BESS in the neighboring areas, according to K_{Bi}^* and K_{Bj}^*. Meanwhile, the charging or discharging of each BESS is also decided. Three scenarios with different K_{Bi}^* and K_{Bj}^* may happen in the power system after disturbances, and details are shown as follows. Additionally, as Δf and ACE in each area keep changing in the process of STCL-AGC, K_B is also variable.

- **Scenario #1:** K_{Bi}^* is less than K_{Bj}^*, and K_{Bi}^* can be zero.

In this scenario, K_{Bi}^* is less than K_{Bj}^*, which means the Area j is with a larger CPS1. In other words, BESS$_j$ under the control of STCL can focus more on the mitigation of ΔP_{tie}, regardless of the recovery of Δf. Thus, the participation factor for both BESS K_B equals to K_{Bj}^*. Meanwhile, the discharging or charging of BESS follows Area i, because the operation of $BESS_i$ must be benefit to the recovery of Δf.

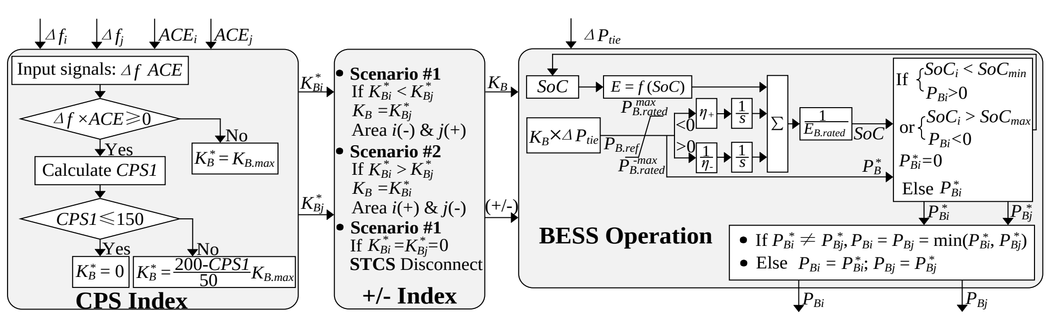

Figure 2. Frameworks of of STCL.

A typical example is used to explain the operation of STCL in this **Scenario #1**. In detail, Δf_i, Δf_j and ΔP_{tie} are negative in the power system for seconds, after an increased load disturbance in Area *i*. Specifically, negative ΔP_{tie} represents that less scheduled power is transferred from Area *i* to Area *j*.

In Area *i*, ACE_i is negative according to (5) and with the same sign of Δf_i. In general, the real time CPS1 is bad, and the participators in Area *i* including BESS must take action to the recovery of Δf_i. The discharging of $BESS_i$ is benefit to the recovery of Δf_i and ΔP_{tie} at the same time. Thus, $BESS_i$ must operate in the discharging mode (-), and the corresponding $BESS_j$ operate in the charging mode (+) if possible.

The situation is different in Area *j*. ACE_j can be positive or negative based on the value of $-\Delta P_{tie}$ and $-B_j\Delta f_j$, according to (6). CPS1 is more than 200%, when $-\Delta P_{tie}$ is larger, and CPS1 is normally more than 150%, even when $-B_j\Delta f_j$ is larger. The participators in this area are unnecessary to take action to avoid the deteriorate of CPS1, and $BESS_j$ can be used to focus on mitigating ΔP_{tie}. However, the charging power of BESS must be carefully concerned, as the operation of $BESS_j$ is against the recovery of Δf_j. Thus, K_B for BESS in both areas equals to K^*_{Bj}.

$$ACE_i = \Delta P_{ij} + B_i\Delta f_i \tag{5}$$

$$ACE_j = -\Delta P_{ij} + B_i\Delta f_j \tag{6}$$

Thus, STCL makes $BESS_i$ discharge power, and $BESS_j$ charge the same amount of power at the same time. The operation of that pair of BESS is definitely benefit to the recovery of ΔP_{tie}. Also, the operation of $BESS_j$ worsens Δf_j, but effectively constrained by monitoring CPS1. As long as CPS1 of *Area j* is not satisfying, **Scenario #1** is shifted.

- **Scenario #2:** K^*_{Bj} is less than K^*_{Bi}, and K^*_{Bj} can be zero.

Scenario #2 is opposite to Scenario #1. According to the operation rule of STCL, the charging or discharging of the BESS in both areas are decided by K^*_{Bj}, which is smaller than K^*_{Bi}. Meanwhile, the participation factor K_B in this Scenario equals to K^*_{Bi}.

- **Scenario #3:** $K^*_{Bi}$and K^*_{Bj} equal to 0.

Scenario #3 represents the situation that both areas suffer disturbances, and the recovery of Δf is positive to the recovery of ΔP_{tie}. The STCL is unnecessary to be involved to mitigate ΔP_{tie}, and the conventional AGC can deal with the problem.

For example, an increased load disturbance and a decreased load disturbance happen in Area *i* and Area *j* respectively. AGC generators supply power in Area *i* and consumer power in Area *j* are positive to the recovery of Δf and ΔP_{tie} at the same time. Thus, the exiting AGC is sufficient in this scenario, and STCL is cut off.

3.3 BESS Operation Block

The process of the 'BESS Operation block' is shown as the left part of Figure 3. As BESS in the neighboring areas share the same participation factor K_B after '+/- Index block' and respond to ΔP_{tie}, a pair of BESS supply or consume the same amount of power (P_{Bi} and P_{Bj}) at the same time.

However, the actual operation of BESS is limited by the characteristics of batteries such as the rated power ($P_{B.rated}$), the rated capacity ($E_{B.rated}$) and *SoC*. First, BESS cannot provide or consume the power less or more than $P^{max}_{B.rated}$ or $P^{-max}_{B.rated}$. Meanwhile, *SoC* must monitored in real time, as SoC must be kept in an acceptable range such as [20%,80%]. In this block, BESS are switched off to avoid the over-charging or over-discharging, when (SoC < SoC_{min} & P_B > 0) and (SoC > SoC_{max} & P_B < 0). Thus, the possible outputs of $BESS_i$ and $BESS_j$ marked as P^*_{Bi} and P^*_{Bj} are generated first. Specifically, the calculation of SoC is shown as (7) and (8).

$$E_B(t_n) = \begin{cases} E_B(t_{n-1}) - \frac{1}{\eta_-} P_B^{>0}(t_n) \times t \\ E_B(t_{n-1}) - \eta_+ P_B^{<0}(t_n) \times t \end{cases} \tag{7}$$

$$SoC(t_n) = SoC(t_{n-1}) \pm \frac{E_B(t_n)}{E_{B.rated}} \tag{8}$$

where $E_B(t_n)$ and $E_B(t_{n-1})$ are the energy stored in BESS at time *t* and *t-1*, $P_B(t_n)$ is the BESS output power (>0 for discharging and <0 for charging); and $\eta_+ = 0.9$ and $\eta_- = 0.95$ are charging and discharging efficiency of BESS respectively.

As BESS in neighboring areas are under the coordinated control, 'BESS Operation block' in the further step makes the final output P_{Bi} and P_{Bj} same. For example, SoC of $BESS_i$ exceeds less than SoC_{min}, and P^*_{Bi} becomes 0. In this case, P_{Bi} and P_{Bj} are both set to be 0.

In summary, with the application of those three steps in real time, STCL can effectively mitigate the fluctuation of ΔP_{tie} in AGC. Moreover, the recovery of Δf in some extend is also improved. Also, the AGC performance in each area is still ensured by monitoring CPS, and the SoC of BESS is guaranteed.

4 DYNAMIC MODEL OF STCL-AGC

IN this section, the dynamic model of STCL-AGC is discussed in the system with two neighboring areas. In the model, the power system is assumed as a linear and time-constant system, and a linearized model is permitted to analyses the load frequency control problem of power system. Also, generators in each area such as reheat thermal generators, hydro generators are assumed to be one equivalent non-reheat turbine generator, and the equivalent model is shown as the 'Dynamic model of generator' block in Figure 3. Specifically, generator responds to $P_{G.ref}$ with the inertia elements T_{Gi} and T_{chi}, due to the governor and the generator response delay. Meanwhile, the primary frequency regulation loop with fixed droop characteristic (R) and the conventional AGC with fixed PI control parameters (K_P and K_I) are considered.

Furthermore, in STCL-AGC model, BESS response in terms of reactive power can be neglected, and the decoupled P-Q control is achieved by the converter control system. After considering those simplifications, the BESS model for the STCL-AGC study can be expressed as the 'Dynamic model of BESS' block. Specifically, BESS respond to $P_{B.ref}$ after an inertial element with respond delay T_B. Thus, the dynamic model of STCL-AGC for two neighboring areas is shown as Figure 3.

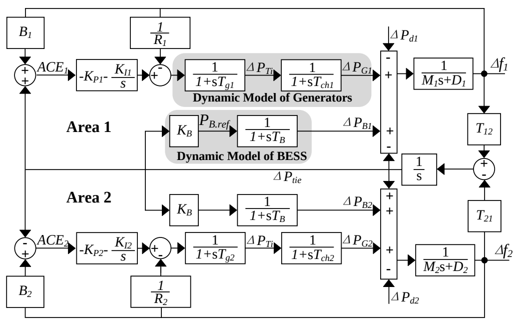

Figure 3. Equivalent model of AGC with STCL in two-area power system.

5 SIMULATION OF STCL

IN this section, case studies are carried out based on a two-area power system. Firstly, $K_{B.max}$ is observed, and three Scenarios are discussed respectively. Moreover, the performance of STCL-AGC is simulated when the system suffers one disturbance and series disturbances. At last, the required sizes of BESS are compared.

The dynamic mode of STCL-AGC has been introduced in Section IV. In detail, Area1 is with 2500MW generation and 2400MW load, and Area2 is with 1900MW generation and 2000 MW load. In this interconnected system, 100MW power flows from Area 1 to Area 2. Meanwhile, the droop characteristics are 5% of each unit. The inertia constant H of every unit is 5 on 100MW base, and the load varies by 1% for a 1% change in frequency. Also the synchronizing torque coefficient T is with a fixed value 1.2, and the C-AGC is with fixed PI parameters. The size of BESS in each area is 25MW/5MWh. Finally, the whole system is calculated in p.u. with 2000MW base, and the corresponding values of parameters in Figure 3 are listed in Table 1 based on Moeini, et. al. (2016) and Delavari, et. al. (2018).

Table 1. Values of parameters of two-area power system (i∈[1,2])

Values	Area 1	Area 2
T_{ch}	0.3	0.4
T_{gi}	0.1	0.17
R_i	0.05	0.05
D_i	1.2	1
β_i	21.2	21
M_i	1385	9.5
K_{Pi}	0.4	0.4
K_{Ii}	0.11	0.11

5.1 Calculation of $K_{B.max}$

In this part, the effective of $K_{B.max}$ is observed, and the BESS is assumed with infinite ability (infinite power and capacity). In this part, for the specific two-area power system, $K_{B.max}$ varies from 0 to 25. Meanwhile, the relationships between $K_{B.max}$ and ΔP_{tie} are shown as Figure 4, when a 0.05% p.u. step load increase happens in Area 2. It is obvious, larger $K_{B.max}$ can mitigate more excursion of ΔP_{tie} in STCL-AGC.

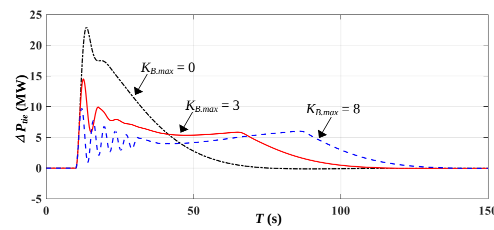

Figure 4. Power fluctuations on tie-line with different $K_{B.max}$.

In conclusion, the larger $K_{B.max}$ can mitigate the excursion of ΔP_{tie}, but brings instability to the system. In addition, the rated power of BESS limits the performance of STCL by the 'BESS operation block', and will be further discussed in Part C.

5.2 Typical Scenario Analysis in STCL-AGC

The choice of Scenarios in the operation of STCL is discussed in this part. To explore the operation of 'CPS Index block' and 'discharging / charging (+/-) Index block', three cases (listed in Table 2) are simulated in the two-area power system. Meanwhile, to avoid the influence of the 'BESS operation block', BESS are still with infinite ability. Also, to make the output of BESS in a reasonable rang, $K_{B.max}$ is set as 5.

Table 2. Three kinds of disturbances

Case #	Details
Case #1	0.05% p.u. load disturbance in Area 2 (t =10s)
Case #2	0.05% p.u. load disturbance in Area 1 (t =10s)
Case #3	0.05% p.u. load disturbances happen in both areas (t =10s)

Specifically, in Case #1, the real time CPS1 of Area 1 and Area 2 are calculated by 'CPS Index block' as Figure 5(a), and the corresponding K_{B1}^* and K_{B2}^* are obtained as Figure 5(a). Moreover, '+/- Index block' decides that STCL operates in Scenario #2, as K_{B1}^{*} is more than K_{B2}^{*}. According to the operation rules, K_B equals to K_{B1}^{*} as Figure 5(c). Meanwhile, BESS in Area 1 are charged and BESS in Area 2 are discharged in Figure 5(d), as ΔP_{tie} follows from Area 1 to Area2.

Similarly, in Case #2, $CPS1_2$ is more than $CPS1_1$ as Figure 6(a), and the corresponding K_{B1}^{*} is less than K_{B2}^{*} as Figure 6(b). STCL operates in Scenario #1. Thus, K_B equals to K_{B2}^{*} as Figure 6(c), and the operation of BESS is shown in Figure 6(d).

At last, in case 3, as $CPS1_1$ and $CPS1_2$ are less than 150%, K_{B1}^{*} and K_{B2}^{*} equal to 0 as Figure 7(a) and Figure 7(b). Thus, STCL operates on Scenario #3. K_B equals 0, and STCL cuts off BESS as Figure 7(c) and Figure 7(d).

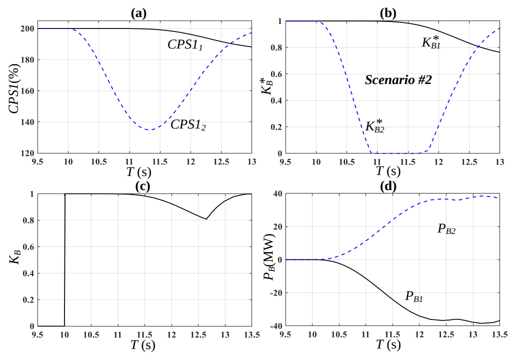

Figure 5. Operation of STCL-AGC in Case #1.

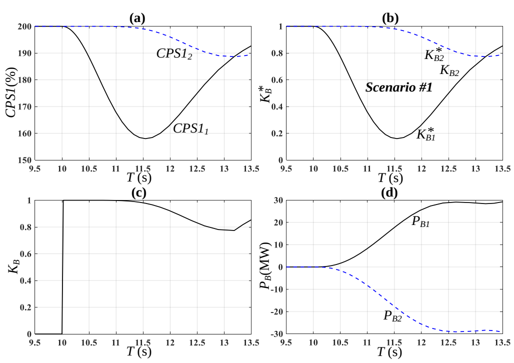

Figure 6 Operation of STCL-AGC of Case #2.

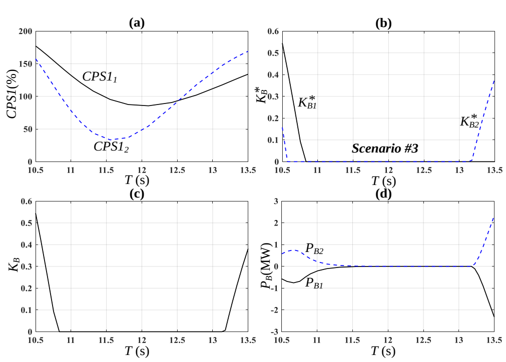

Figure 7. Operation of STCL-AGC of Case #3.

5.3 Performance of ACG with STCL

The system performance under the C-AGC and STCL-AGC are compared in this part. In the simulation, 'BESS operation block' are fully considered, and BESS cannot provide more power than the rated power (25MW). Also, one load disturbance and series disturbances are considered in the system respectively.

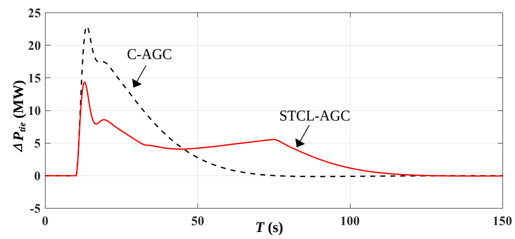

Figure 8. Tie-line power excursion under AGC with STCL.

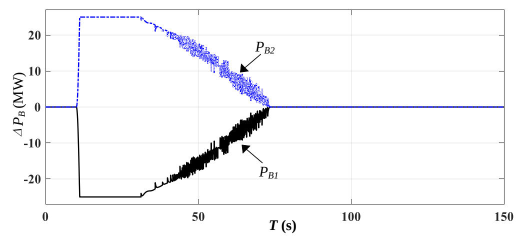

Figure 9. BESS outputs in both Areas.

First, a 0.05% p.u. step increase load disturbance happens in Area 2. The tie-line fluctuations are shown as Figure 8. In detail, the black dotted line represents ΔP_{tie} from Area 1 to Area 2 under the C-AGC with the peak excursion about 25MW. Nevertheless, with the application of STCL-AGC, ΔP_{tie} effectively decreases with the peak excursion about 15MW. Thus, STCL mitigates the power fluctuations on the tie-line, and further releases the risks of the power over-loading.

Moreover, *BESS₁* charge power in Area 1, and *BESS₂* discharge the same amount of power in Area 2 as in Figure 9. As BESS do not take responsibility of the mismatches between load and generation, BESS reach their maximum power and operation for a period, but finally go back to zero. The AGC generators gradually increase their output power to compensate the power mismatches.

Furthermore, the frequency deviations in both areas Δf_1 and Δf_2 are shown as Figure 10. When STCL is applied in the AGC, Δf_1 becomes worse, as the charging of $BESS_1$ brings more disturbances in Area 1. However, as indicated in the black curve in Figure 11, the real-time CPS1 values of Area 1 are all above 190%. In other words, the increase of Δf_1 is acceptable in the exiting CPS. Meanwhile, Δf_2 becomes better, as the fast discharging of BESS in Area 2. Hence, STCL scarifies the frequency recovery in Area 1 to improve the performance of Δf_2 and mitigate ΔP_{tie}.

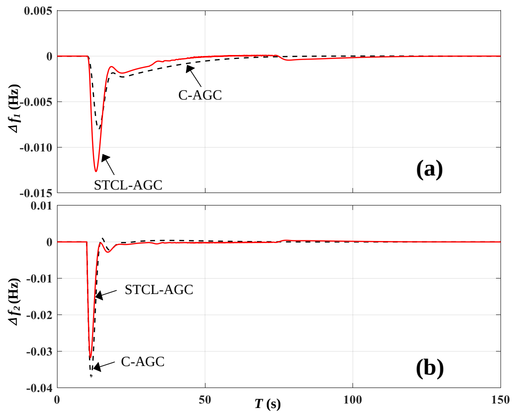

Figure 10. **BESS outputs in both Areas.**

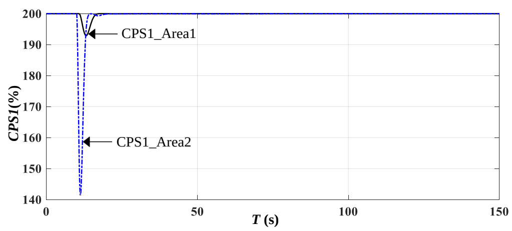

Figure 11. **CPS1 values of both Areas.**

In summary, STCL-AGC provides a better balancing between the frequency recovery and tie-line recovery in AGC. A small amount of power is regarded only transferred between BESS in neighboring areas without participating AGC. Nevertheless, ΔP_{tie} is with a fewer excursions of the scheduled power flow, and CPS always meet the requirements. Finally, the performance of AGC improved.

6 CONCLUSIONS

THE stability of system frequency is the major consideration in the C-AGC, and the power support between areas are encouraged. However, with the trend of deregulation, to mitigate the unscheduled power exchange gets more attention. In this paper, STCL-AGC is proposed to balance the recovery of Δf and ΔP_{tie} with monitoring CPS. Meanwhile, BESS in the proposed control strategy do not perform as generators which take the responsibility of the load and generation mismatch. In this way, BESS only replace the generators in a short period before the conventional generators finish their AGC, as BESS are with fast response time. Therefore, STCL-AGC can improve the AGC performance with small size of BESS, and can be used in practical.

In addition, the control strategy will be further developed in the following research. For example, the STCL will be extended from two neighboring areas to multiple neighboring areas. Meanwhile, the renewable energy generators are considered as well, because the renewable energy transmission between areas becomes common in the further. At last, the controller itself can be further improved to decrease the damping.

7 ACKNOWLEDGMENT

THIS work is supported by a Grant for Key Research and development program of Jiangsu Province (BE2015157), the Fundamental Research Funds for the Central Universities (2242016R20004).

8 REFERENCES AND FOOTNOTES

Avila, T., H. Chavez, (2016). *Secondary reserves determination based on cps1 and cps2 compliant agc operation, ieee international conference on automatica*. 1-5.

Bevrani, H., Y. Mitani and K. Tsuji, (2004). *Robust decentralised load-frequency control using an iterative linear matrix inqualities algorithm, IEE Proc.- Gener. Transm. Distrib.* 151(3), 347-354.

Chen, S., T. Zhang, H. B. Gooi, R. D. Masiello and W. Katzenstein, (2016). *Penetration rate and effectiveness studies of aggregated BESS for frequency regulation, IEEE Trans on Smart Grid.*7(1), 167-177.

Cheng, Y., M. Tabrizi, A. Povedano and D. Nichols, (2014). *Dynamic Available AGC Based Approach for Enhancing Utility Scale Energy Storage Performance, IEEE Trans on Smart Grid*. 5(2), 1070-1078.

Christie, R., A. Bose, (2007). *Load frequency control issues in power system operations after deregulation, Control Systems for Live Entertainment*. 11(3), 18 – 23

Delavari, A.. I. Kamwa, (2018). *Improved optimal decentralized load modulation for power system primary frequency regulation, IEEE Transactions on Power Systems*. 33(1), 1013-1025.

Delille, G.. B. Francois, G. Malarange, (2012). *Dynamic frequency control support by energy storage to reduce the impact of wind and solar generation on isolated power system inertia, IEEE Transactions on Sustainable Energy*. 3(4), 931-939.

Dianjie Lu, Xiaoxia Huang, Guijuan Zhang, Xiangwei Zheng, Hong Liu. (2018)Trusted Device-to-Device based Heterogeneous Cellular Networks: A New Framework for Connectivity Optimization, IEEE Transactions on Vehicular Technology, 67(11):11219-11233.

Dong, X.. C. Wang, Z. Yun, Y. Wang, P. Zhao, Y. Ding, (2017). *Power flow analysis considering automatic generation control for multi-area interconnection power networks, IEEE Transactions on Industry Applications*. 1-10

Farahani, M., S. Ganjefar and M. Alizadeh, (2012). *PID controller adjustment using chaotic optimisation algorithm for multi-area load frequency control, IET Control Theory Appl.* 6(13), 1984-1992.

Kottick, D.. M. Blau, D. Edelstein, (1993). *Battery energy storage for frequency regulation in an island power system, IEEE Transactions on Energy Conversion*. 8(3), 455-459.

Kundur, P. (1994). *Power System stability and contol, McGraw-Hill Education*.

Kung, C. H.. M. Devaney, C. Huang, C. Kung, (1998). *Fuzzy-based adaptive digital power metering using a genetic algorithm, IEEE Instrumentation & Measurement Technology Conference*. IEEE.

Ma, M., C. Zhang, X. Liu, C. Hong, (2017). *Distributed model predictive load frequency control of multi-area power system after deregulation, IEEE Transactions on Industrial Electronics*. 64(6), 1-1.

Mercier, P., R. Cherkaoui, A. Oudalov, (2009). *Optimizing a battery energy storage system for frequency control application in an isolated power system, IEEE Transactions on Power Systems.* 24(3), 1469-1477.

Mi, Y., Y. Fu, C. Wnag and P. Wang, (2013). *Decentralized sliding mode load frequency control for multi-area power systems, IEEE Trans on Power Syst.* 28(4), 4301-4309.

Miao, L., J. Wen, H. Xie, C. Yue and W. J. Lee, (2015). *Coordinated control strategy of wind turbine generator and energy storage equipment for frequency support, IEEE Trans on Industry Applications*. 51(4), 2732-2742.

Moeini, A., I. Kamwa, (2016). *Analytical concepts for reactive power based primary frequency control in power systems, IEEE Transactions on Power Systems*. 31(6), 1-14.

Mohanty, P. K., B. K. Sahu, T. K. Pati, S. Panda and S. K. Kar, (2016). *Design and analysis of fuzzy PID controller with derivative filter for AGC in multi-area interconnected power system, IET Gener. Trans.& Distrib*. 10(15), 3764-3776.

Olmos, L., J. Fuente, J. Macho, R. Pecharromán, A. Calmarza and J. Moreno, (2004). *New design for the Spanish AGC scheme using an adaptive gain controller, IEEE Trans on Power Syst.* 19(3),1528-1537.

Pan, I. & S. Das, (2016). *Fractional order AGC for distributed resources using robust optimization, IEEE Trans on Smart Grid.* 7(5), 2175-2185.

Rerkpreedapong, D., A. Hasanovic and A. Feliachi, (2003). *Robust load frequency control using genetic algorithms and linear matrix inequalities, IEEE Trans on Power Syst.* 18(2), 855-861.

Sharma, S. & B. Singh, (2014). *Asynchronous Generator With Battery Storage for Standalone Wind Energy Conversion System, IEEE Trans on Industry Applications*. 50(4), 2760 - 2767.

Sui, X., Y. Tang, H. He, J. Wen, (2014). *Energy-storage-based low-frequency oscillation damping control using particle swarm optimization and heuristic dynamic programming, IEEE Transactions on Power Systems.* 29(5), 2539-2548.

Tabarez, J. & S. Ranade. (2016). *A proposed energy storage controller for mitigating impact of wind farms on AGC, in North American Power Symposium, Denver, CO, USA.*

Tan, W. (2010). *Unified tuning of PID load frequency controller for power systems via IMC, IEEE Trans on Power Syst.* 25(1), 341-350.

Yang, A.M.; Yang, X.L.; Chang, J.C.; Bai, B.; Kong, F.B.; Ran, Q.B. (2018).Research on a fusion scheme of cellular network and wireless sensor networks for cyber physical social systems. Ieee Access, 6(99): 18786-18794.

Zhou, X., Liang, X., Du, X., & Zhao, J. (2018). Structure based user identification across social networks. IEEE Transactions on Knowledge and Data Engineering, 30(6), 1178-119

9 DISCLOSURE STATEMENT

NO potential conflict of interest was reported by the authors.

10 NOTES ON CONTRIBUTORS

Shengqi Zhang received the B.E. degree in electrical engineering and automation from Southeast University, China, in 2010, the M.E. degree in electrical engineering from the University of Queensland, Australia, 2012, and the Ph.D. degree in the Power Engineering field from Queensland University of Technology, 2016. His research interests include renewable energy generator, energy storage system, and system frequency respond. His contribution of this paper includes writing original draft preparation.

Bei Yuan received the B.E. degree in electrical engineering and automation from Hohai University, China, in 2016. Currently, she is the master student of the School of Electrical Engineering, Southeast University. Her research field is the optimization and application of BESS in smart grid. Her contribution of this paper includes writing original draft preparation.

Jianfeng Zhao received the B.S. degree from Huainan Mining Institute, Huainan, China, the M.S. degree from Nanjing University of Aeronautics and Astronautics, Nanjing, China, and the Ph.D. degree from Southeast University, Nanjing, in 1995, 1998,and 2001, respectively, in electrical engineering. Currently, he is the Professor of the School of Electrical Engineering, Southeast University, and he has been engaged in teaching and research in the field of high-power electronics. He has published more than 90 papers and 22 China invention patents. His research interests are utility applications of power electronics in smart grid such as solid-state transformer, active filters for power conditioning, flexible ac transmission system devices, multilevel ac motor drives, and efficient energy utilization. His contribution of this paper includes writing-review and editing.